Chem. Chem. Technol., 2025, Vol. 19, No. 3, pp. 447–454 Chemistry

SONOCHEMICAL SYNTHESIS, CHARACTERIZATION, AND ANTIBACTERIAL ACTIVITY INVESTIGATION OF COPPER OXIDE NANOPARTICLES/CLINOPTILOLITE COMPOSITE

Yuriy Sukhatskiy^{1, ⊠}, Roman Mnykh¹, Iryna Tymchuk², Martyn Sozanskyi¹, Marian Matskiv¹, Zenovii Znak¹, Mariana Shepida¹, Artur Mazur¹

https://doi.org/10.23939/chcht19.03.447

Abstract. CuO nanoparticles (NPs)/clinoptilolite composite was obtained via sonochemical synthesis using copper sulfate as a precursor and sodium hydroxide as a precipitating agent. The synthesized composite was characterized by XRD, EDX, FTIR, and SEM techniques. High antibacterial activity of the composite against the grampositive bacterium *Staphylococcus aureus* subsp. *aureus* ATCC 25923 was established.

Keywords: sonochemical synthesis, CuO nanopartic-les/clinoptilolite composite, Debye–Scherrer equation, antibacterial activity, gram-positive bacterium *Staphylococcus aureus*.

1. Introduction

Natural zeolites are hydrated porous crystalline aluminosilicate materials¹ containing pores of various sizes, ranging from micropores (size <2 nm) to macropores (size >50 nm).² Primarily, natural zeolites are formed from volcanic and sedimentary rocks, such as chabazite, mordenite, and clinoptilolite.3 The three-dimensional framework of zeolites consists of TO₄ tetrahedra (where T - tetrahedrally coordinated Si, Al, or P) connected by sharing an oxygen atom.^{4,5} The tetrahedrally coordinated Al atoms cause the occurrence of negative charges in the zeolite framework, which are neutralized by out-offramework cationic species.⁶ The empirical formula of the zeolite can be represented as $Ma/b[(AlO_2)_a(SiO_2)_v] \cdot cH_2O$, where M is an alkali or alkaline earth metal cation, b is the valence of the metal cation, a and y are the total number of [SiO₄]⁴⁻ and [AlO₄]⁵⁻ tetrahedra in the zeolite unit cell, and c is the amount of crystallization water per unit cell.⁷

Zeolites can act as molecular sieves due to their porous structure, and also can selectively adsorb and separate guest species of different shapes, sizes, and polarities. The combination of the porous structure of zeolites with catalytically active centers in their frameworks allows their use as shape-selective catalysts for the controlled synthesis of chemical compounds. The main advantages of zeolites, which lead to their wide range of practical applications, are high thermal stability, controllable acidity, and, accordingly, non-corrosive behaviour, biocompatibility, the absence of disposal problems, and low prime cost. Key global producers of natural zeolite include China, South Korea, and Slovakia.

The Si/Al ratio in a zeolite determines its ion-exchange capacity. ¹⁰ Erdem *et al.* ¹¹ reported that the sorption of heavy metal cations on natural zeolite occurs in the following order: Co²⁺>Cu²⁺>Zn²⁺>Mn²⁺. The unique properties of zeolites make their use in water treatment technologies, ¹² for gas adsorption, ¹³ green chemistry, ¹⁴ for catalytic production of aromatic compounds and green fuels from non-petroleum carbon-based resources (including CH₃OH, CO, CO₂, and biomass ^{15,16}), as feed additives for animals ¹⁷, and in medicine (in modern drug delivery systems, as engineered frameworks for tissue engineering, antibacterial agents, wound healing, implant coatings, filling of tooth root canals, *etc.*)^{10, 18}.

Inorganic compound nanoparticles, particularly transition metal oxide nanoparticles, are much more stable than organic compound nanoparticles. ¹⁹ Copper oxide (CuO) is a p-type semiconductor with a narrow band gap (ranging from 1.2 to 1.9 eV). ²⁰ Compared to other transition metal oxides, the advantages of copper oxide include availability, lower cost, ²¹ good electrical properties, low thermal emittance, and high solar absorbance. ²² Copper oxide nanoparticles (CuO NPs) exhibit a high surface-to-volume ratio, ²³ which provides high antibacterial, antioxidant, antifungal, and anticancer potentials by reactive oxygen species and copper-ion release mechanisms. ^{24,25} The most common reactive species that

 $^{^{\}rm I}$ Lviv Polytechnic National University, 12 S. Bandery St., Lviv 79013, Ukraine

² Danylo Halytsky Lviv National Medical University, 69 Pekarska St., Lviv 79010, Ukraine

[™] yurii.v.sukhatskyi@lpnu.ua

[©] Sukhatskiy Y., Mnykh R., Tymchuk I., Sozanskyi M., Matskiv M., Znak Z., Shepida M., Mazur A., 2025

chemically degrade bacterial cell walls are hydroxyl radicals and hydroxide ions. ²⁶⁻³⁰

The industrial applications of CuO, including that in the nanoparticle form, are diverse. ^{21,22,26,31-33} It is used as a catalyst in chemical syntheses; as bio-sensors and gas sensors; in the development of lithium-ion batteries and supercapacitors; for the fabrication of solar cells; in water purification for the removal of organic pollutants and heavy metal ions; in photocatalysis; in agriculture for the development of nano-fertilizers with prolonged and controlled release of active elements; and in biomedicine (including antimicrobial, antifungal, antibiotic, anti-inflammatory, antioxidant, anticancer, and drug delivery applications). The main methods for synthesizing CuO NPs include hydro- and solvothermal, sol-gel, co-precipitation, microemulsion, and microwave irradiation. ^{19,34}

The aim of the work was to investigate the structural and phase characteristics of CuO NPs/clinoptilolite composite synthesized by the sonochemical method and its antibacterial activity.

2. Experimental

2.1. Materials and chemicals

To obtain CuO NPs/clinoptilolite composite, natural clinoptilolite from the Sokyrnytsia deposit (Transcarpathian region, Ukraine) with particle sizes ranging from 0.063 to 0.1 mm was used. Copper sulfate (CuSO₄·5H₂O) and 2 M aqueous solution of sodium hydroxide (NaOH) were purchased from Merck. All reagents were of analytical grade purity and were used without additional purification procedures. Distilled water was used to prepare the solutions. A strain of gram-positive bacteria, *Staphylococcus aureus* subsp. *aureus* ATCC 25923, was provided by Danylo Halytsky Lviv National Medical University.

2.2. Sonochemical synthesis of CuO NPs/clinoptilolite composite

We prepared 300 mL of an aqueous $CuSO_4$ solution with a concentration of 10 wt%. Then, 20 g of natural clinoptilolite was added to the solution. The resulting suspension was stirred (frequency - 300 rpm) at a temperature of 80 °C for 5 h to provide ion exchange between Cu^{2+} ions from the solution and exchangeable cations in the clinoptilolite. CuO precipitation was carried out by adding a 2 M NaOH solution until pH=11 was reached. Simultaneously with the NaOH addition, the suspension was treated for 10 min in an ultrasonic (US) cavitation field (device for generating cavitation phenomena – Bandelin Sonopuls HD 2200.2 generator; US

power density – 200 W/L; US frequency – 20 kHz). During this process, a color change in the dispersion medium from blue to black was observed. After 2 h of stirring (frequency – 300 rpm), the synthesized product (CuO NPs/clinoptilolite composite) was separated from the liquid phase by filtration, washed three times with distilled water, and dried for 12 h at a temperature of 110 °C.

2.3. Characterization of CuO NPs/clinoptilolite composite

The phase composition of the synthesized composite was determined by X-ray diffraction (XRD) using an AERIS Research diffractometer with CuK_{α} radiation. The average crystallite size (D, nm) of the CuO NPs was calculated by the Debye–Scherrer equation:²²

$$D = \frac{k\lambda}{\beta\cos\theta},\tag{1}$$

where k = 0.94 is the Scherrer coefficient; $\lambda = 0.154$ nm is the wavelength of the X-ray radiation; β is the full width at half maximum of the reflection peaks, rad; and θ is the diffraction angle, rad.

The elemental composition of the composite surface was confirmed by energy-dispersive X-ray analysis (EDX) on an INCA Energy 350. Inductively coupled plasma mass spectrometry (ICP-MS) analyses were performed with a 7850 ICP-MS spectrometer (Agilent Technologies) to determine the accurate content of Cu, Al, and Si. The identification of the functional groups of chemical bonds was performed using FTIR spectra recorded on a Spectrum Two spectrophotometer (the range of 400–4000 cm⁻¹). The surface morphology of the obtained composite was investigated, and the weighted average size of the CuO NPs was evaluated by scanning electron microscopy (SEM) on a ZEISS EVO 40XVP microscope.

2.4. Antibacterial activity of CuO NPs/clinoptilolite composite

The antibacterial activity of CuO NPs/clinoptilolite composite against the gram-positive bacterium *Staphylococcus aureus* subsp. *aureus* ATCC 25923 was determined by adding 1 mL of a pure culture suspension of the microorganism, standardized to the 0.5 McFarland standard (approximately 1.5×10⁸ cells), to the composite samples weighing 0.01 g and 0.1 g, respectively. After mixing CuO NPs/clinoptilolite composite with the *Staphylococcus aureus* subsp. *aureus* ATCC 25923 suspension, sowings were made using disposable bacteriological loops (with a volume of 10 μL) onto a solid nutrient medium (Hottinger agar) after 5, 10, 30, and 60 min, as well as after 24 h of contact between the composite and the microorganism strain. A control of bacterial growth

was also conducted without adding the composite to the pure culture suspension of the microorganism. Cups with sowings were incubated in a thermostat at 37 °C for 24 h. After that, the number of colonies of the studied microorganism (the number of colony-forming units) that grew on the nutrient medium was counted.

3. Results and Discussion

3.1. Characterization of CuO NPs/clinoptilolite composite

The US-assisted formation of CuO NPs/clinoptilolite composite using copper sulfate as a precursor and sodium hydroxide as a precipitating agent can be represented by the following reactions:

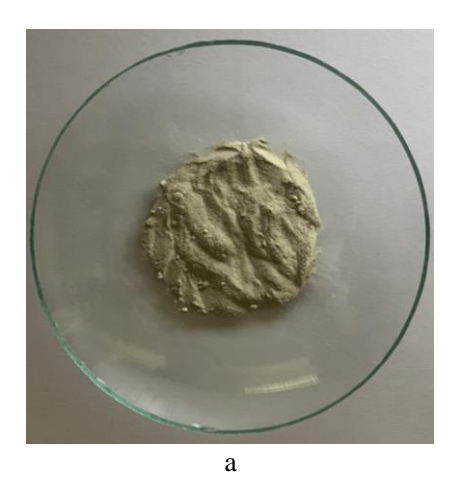
$$2\text{Me}^+/\text{clinoptilolite} + +\text{Cu}^{2+} \rightarrow \text{Cu}^{2+}/\text{clinoptilolite} + 2\text{Me}^+,$$
 (2)

or
$$Me^{2+}$$
/clinoptilolite +
+ $Cu^{2+} \rightarrow Cu^{2+}$ /clinoptilolite + Me^{2+} , (3)

$$Cu(OH)_2/clinoptilolite \xrightarrow{t})))$$

$$CuO NPs/clinoptilolite + H_2O,$$
(5)

where Me^+ is an alkali metal cation, Me^{2+} is an alkaline earth metal cation.



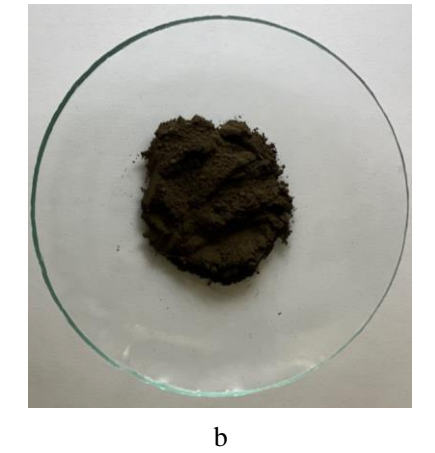


Fig. 1. Photographs of (a) clinoptilolite, and (b) CuO NPs/clinoptilolite composite

Photographs of clinoptilolite and CuO NPs/clinoptilolite composite are presented in Fig. 1. As seen in Fig. 1b, the synthesized CuO NPs/clinoptilolite composite was black, confirming the presence of CuO NPs in the clinoptilolite framework.

XRD patterns of clinoptilolite and CuO NPs/clinoptilolite composite are shown in Fig. 2. The clinoptilolite pattern (Fig. 2a) reveals peaks corresponding to the monoclinic structure of clinoptilolite (space group C2/m), ³⁵ and after CuO NPs precipitation (Fig. 2b), the patterns in the range of $2\theta = 10^{\circ}-30^{\circ}$ are similar. This indicates that the structure of clinoptilolite was not changed. However, the intensity of the clinoptilolite peaks in Fig. 2b decreased compared to Fig. 2a, and new diffraction peaks appeared in the range of $2\theta = 32^{\circ}-75^{\circ}$, corresponding to the (110), (002), (111), (020), (202), (022), (220), (311), and (004) planes of monoclinic CuO (space group C2/c; JCPDS No. $(45-0937)^{23}$. The lattice parameters were a = 4.694(1) Å, b= 3.396(1) Å, c = 5.135(1) Å, and $\beta = 99.538(1)^{\circ}$. The average crystallite size of CuO NPs, calculated by the Debye–Scherrer equation at $2\theta = 35.686^{\circ}$, was about 14

nm. The absence of other peaks characteristic of secondary phases (impurities) confirmed the high purity of the synthesized product.

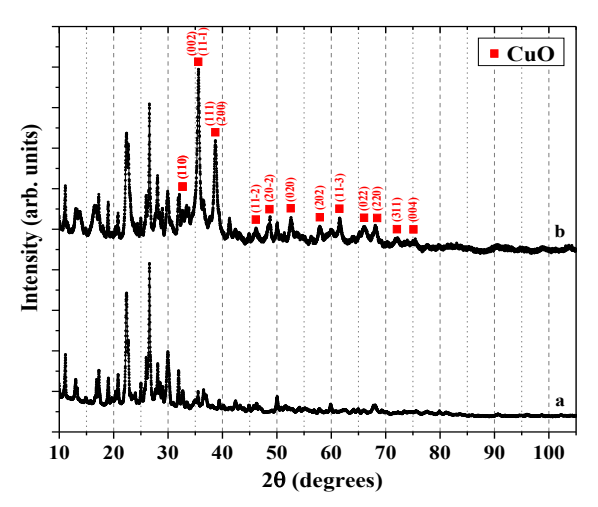


Fig. 2. XRD patterns of (a) clinoptilolite, and (b) CuO NPs/clinoptilolite composite

The EDX spectrum of the final product (Fig. 3) showed that, in addition to the peaks of elements such as Al, Si, and O, characteristic of the natural aluminosilicate (clinoptilolite), new peaks appeared at 1.0, 8.1, and

8.9 keV, which correspond to Cu. This indicated that CuO NPs were immobilized in the clinoptilolite framework. The surface Cu content in the synthesized composite was 53.60 wt% (Table 1).

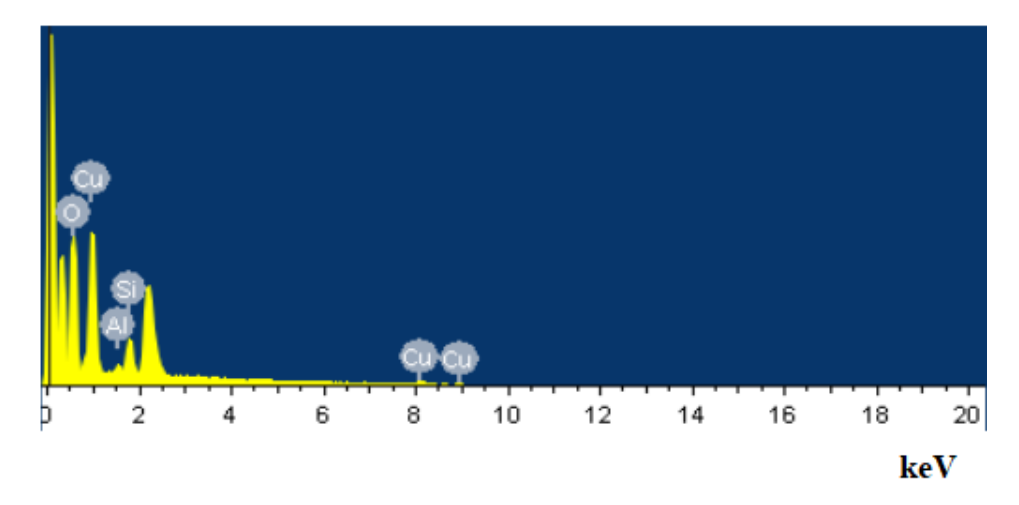


Fig. 3. EDX spectrum of CuO NPs/clinoptilolite composite

Table 1. The elemental composition of the surface of CuO NPs/clinoptilolite composite

Element	Weight%	Atomic%	
О	38.33	67.90	
Al	1.13	1.19	
Si	6.94	7.00	
Cu	53.60	23.91	
Totals	100.00	100.00	

The Cu content determined by ICP-MS measurements was 4.52 wt%, and the molar Si/Al ratio was 5.15.

Fig. 4 presents the FTIR spectra of clinoptilolite and CuO NPs/clinoptilolite composite recorded in the range of 400–4000 cm⁻¹. The vibration bands at 3387–3398 cm⁻¹ and 1628–1631 cm⁻¹ can be attributed, respectively, to the stretching vibration of the surface O–H groups adsorbed on the CuO NPs surface, and to the bending and stretching vibrations of H₂O molecules.^{22,24,34} The bands at 1012–1085 cm⁻¹ are attributed to the internal linkages between [SiO₄]⁴⁻ and [AlO₄]⁵⁻ tetrahedra in the clinoptilolite framework.³⁶ In the low-frequency region (at 441–947 cm⁻¹), the symmetric stretch vibrational modes of Si–O–Si and Si–O–Al groups were concentrated.²⁶ The characteristic peak at 416 cm⁻¹ corresponds to the stretching vibrations of Cu–O.²⁴

As a result of the interaction between CuO NPs and the clinoptilolite framework,²² bathochromic (red) shifts (from 1628 to 1631 cm⁻¹, from 1012 to 1085 cm⁻¹, and from 777 to 779 cm⁻¹), hypsochromic (blue) shifts (from 3398 to

3387 cm⁻¹ and from 597 to 596 cm⁻¹), as well as the appearance of a peak at 416 cm⁻¹, were observed in the FTIR spectrum of the composite (Fig. 4).

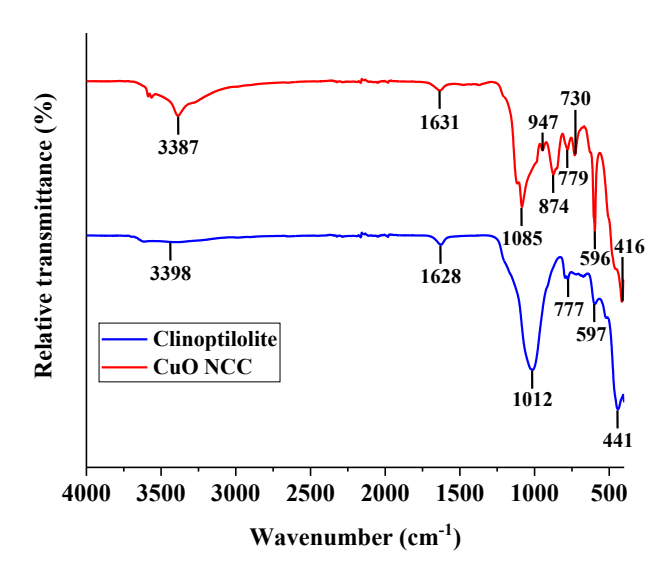
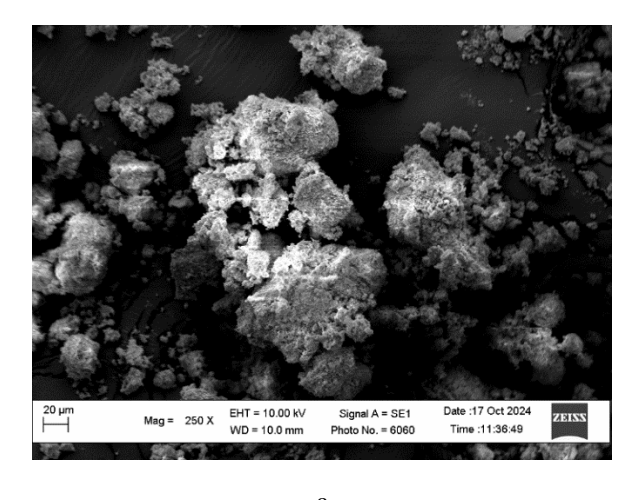


Fig. 4. FTIR spectra of clinoptilolite and CuO NPs/clinoptilolite composite

From Fig. 5, it can be seen that the surface of clinoptilolite was uniformly covered with slightly agglomerated granular CuO particles, 70% of which had sizes from 60 to 100 nm. Using specialized software (Carl Zeiss Vision AxioVision Viewer 4.8), the weighted average size of CuO NPs was calculated to be 85.4 nm.



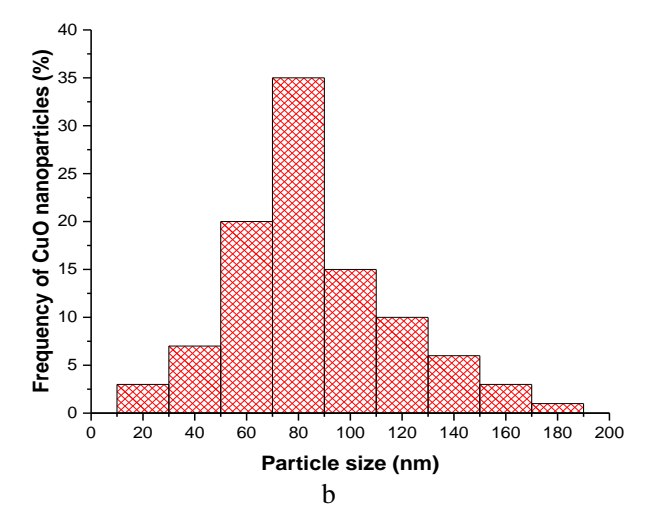


Fig. 5. SEM image of (a) CuO NPs/clinoptilolite composite, and (b) corresponding histogram of particle size distribution

3.2. Antibacterial activity of CuO NPs/clinoptilolite composite

Zeolites modified with transition metal ions (e.g., Ag⁺, Cu²⁺, Zn²⁺, Fe²⁺) have broad-spectrum antimicrobial activity, particularly against gram-positive and gramnegative bacteria.³⁷⁻⁴² The negative charge of pure zeolite cannot neutralise the negative charges of bacterial cell walls. Milenković *et al.*⁴³ reported the effectiveness of Cuexchanged zeolite against *E. coli*. The antibacterial activity of CuO NPs is manifested in the generation of reactive

oxygen species, which, by destroying bacterial cell membranes, penetrate the cells, inhibit their growth, and also potentially cause cell death.⁴⁴ The production of Cu ions significantly contributes to oxidative stress by accumulating reactive oxygen species, including superoxides and hydroxyl radicals. They disrupt processes such as DNA replication, cell division, and metabolism.²¹

The antibacterial activity of CuO NPs/clinoptilolite composite against the gram-positive bacterium *Staphylococcus aureus* subsp. *aureus* ATCC 25923 is presented in Fig. 6 and Table 2.



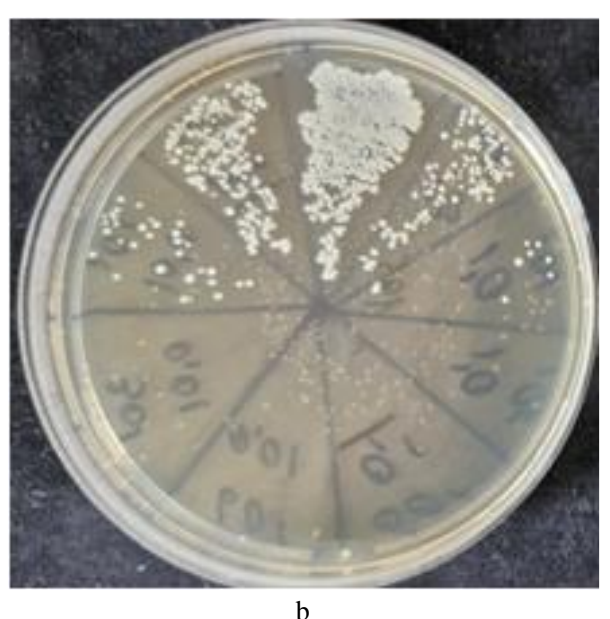


Fig. 6. Photographs of the growth of *Staphylococcus aureus* subsp. *aureus* ATCC 25923 on Hottinger agar plates: (a) top view, and (b) bottom view

It was established that the effectiveness of the antibacterial activity of CuO NPs/clinoptilolite composite

depended on the duration of exposure. At both composite concentrations (0.01 and 0.1 g/mL), the number of CFUs

decreased as early as 5 min of exposure (Table 2). After 30 min of contact between the composite and the strain of *Staphylococcus aureus* subsp. *aureus* ATCC 25923, no live bacteria were detected.

In contrast, in the control experiment without adding the composite to the suspension, continuous growth of microorganisms was observed, making it impossible to count CFUs.

Table 2. Change in the number of CFUs depending on the duration of exposure at different concentrations of CuO NPs/clinoptilolite composite

Concentration of CuO NPs/clinoptilolite	Number of CFUs per exposure duration				
composite, g/mL	5 min	10 min	30 min	60 min	24 h
0.01	229	34	0	0	0
0.1	106	8	0	0	0

4. Conclusions

By the method of sonochemical synthesis using copper sulfate as a precursor and sodium hydroxide as a precipitating agent, we obtained CuO NPs/clinoptilolite composite. The XRD patterns of CuO NPs/clinoptilolite composite showed the presence of peaks characteristic of the monoclinic structure of clinoptilolite and monoclinic CuO. The average crystallite size of CuO NPs, calculated by the Debye-Scherrer equation, was about 14 nm. Confirmation of the presence of CuO NPs in the clinoptilolite framework was the detection of bathochromic (red) and hypsochromic (blue) peak shifts in the FTIR spectrum of the composite, compared to their positions in the FTIR spectrum of pure clinoptilolite. The weighted average size of CuO NPs, determined based on the SEM image of CuO NPs/clinoptilolite composite, was 85.4 nm. The obtained composite showed high antibacterial activity against the gram-positive bacterium Staphylococcus aureus subsp. aureus ATCC 25923. In particular, no live bacteria were detected after 30 min of contact between the composite and the Staphylococcus aureus subsp. aureus strain, at both concentrations of the composite (0.01 and 0.1 g/mL). Thus, the synthesized CuO NPs/clinoptilolite composite has great potential for use as an antibacterial agent.

Acknowledgements

The authors acknowledge the funding of the Ministry of Education and Science of Ukraine for the scientific research project of young scientists "Advanced oxidation processes, including nanocatalytic, based on cavitation technologies for purification of aqueous media from resistant N-substituted organic compounds" (state registration number 0122U000790).

References

[1] Velarde, L.; Nabavi, M.S.; Escalera, E.; Antti, M.-L.; Akhtar, F. Adsorption of Heavy Metals on Natural Zeolites: A Review. *Chemosphere* **2023**, *328*, 138508. https://doi.org/10.1016/j.chemosphere.2023.138508

- [2] Narayanan, S.; Tamizhdurai, P.; Mangesh, V.L.; Ragupathi, C.; Santhana krishnan, P.; Ramesh, A. Recent Advances in the Synthesis and Applications of Mordenite Zeolite Review. *RSC Adv.* **2021**, *11*, 250–267. https://doi.org/10.1039/D0RA09434J
- [3] Derbe, T.; Temesgen, S.; Bitew, M. A Short Review on Synthesis, Characterization, and Applications of Zeolites. *Adv. Mater. Sci. Eng.* **2021**, 2021, 6637898. https://doi.org/10.1155/2021/6637898
- [4] Li, Y.; Yu, J. Emerging Applications of Zeolites in Catalysis, Separation and Host–Guest Assembly. *Nat. Rev. Mater.* **2021**, *6*, 1156–1174. https://doi.org/10.1038/s41578-021-00347-3 [5] Bensafi, B.; Chouat, N.; Djafri, F. The Universal Zeolite ZSM-5: Structure and Synthesis Strategies. A Review. *Coord. Chem. Rev.* **2023**, *496*, 215397.

https://doi.org/10.1016/j.ccr.2023.215397

[6] Pérez-Botella, E.; Valencia, S.; Rey, F. Zeolites in Adsorption Processes: State of the Art and Future Prospects. *Chem. Rev.* **2022**, *122*, 17647–17695.

https://doi.org/10.1021/acs.chemrev.2c00140

[7] Khaleque, A.; Alam, M.M.; Hoque, M.; Mondal, S.; Haider, J.B.; Xu, B.; Johir, M.A.H.; Karmakar, A.K.; Zhou, J.L.; Ahmed, M.B.; Moni, M.A. Zeolite Synthesis from Low-Cost Materials and Environmental Applications: A Review. *Environ. Adv.* **2020**, *2*, 100019.

https://doi.org/10.1016/j.envadv.2020.100019

- [8] Moliner, M.; Martínez, C.; Corma, A. Multipore Zeolites: Synthesis and Catalytic Applications. *Angew. Chem. Int. Ed.* **2015**, *54*, 3560–3579. https://doi.org/10.1002/anie.201406344
- [9] Soonmin, H. Zeolite: Review of Characterization and Applications. *Int. J. Chem. Biochem. Sci.* 2023, 24, 704–715.
 [10] Kraljević Pavelić, S.; Simović Medica, J.; Gumbarević,

D.; Filošević, A.; Pržulj, N.; Pavelić, K. Critical Review on Zeolite Clinoptilolite Safety and Medical Applications *in vivo*. *Front Pharmacol.* **2018**, *9*, 1350.

https://doi.org/10.3389/fphar.2018.01350

- [11] Erdem, E.; Karapinar, N.; Donat, R. The Removal of Heavy Metal Cations by Natural Zeolites. *J. Colloid Interface Sci.* **2004**, 280, 309–314. https://doi.org/10.1016/j.jcis.2004.08.028
- [12] Inglezakis, V.J. The Concept of "Capacity" in Zeolite Ion Exchange Systems. *J. Colloid Interface Sci.* **2005**, *281*, 68–79. https://doi.org/10.1016/j.jcis.2004.08.082
- [13] Poursaeidesfahani, A.; Andres-Garcia, E.; de Lange, M.; Torres-Knoop, A.; Rigutto, M.; Nair, N.; Kapteijn, F.; Gascon, J.; Dubbeldam, D.; Vlugt, T.J.H. Prediction of Adsorption Isotherms from breakthrough Curves. *Microporous Mesoporous Mater*. **2019**, 277, 237–244.

https://doi.org/10.1016/j.micromeso.2018.10.037

- [14] Lima, C.G.S.; Moreira, N.M.; Paixão, M.W.; Corrêa, A.G. Heterogenous Green Catalysis: Application of Zeolites on Multicomponent Reactions. *Curr. Opin. Green Sustain. Chem.* **2019**, *15*, 7–12. https://doi.org/10.1016/j.cogsc.2018.07.006
- [15] Makertihartha, I.G.B.N.; Azhari, N.J.; Kadja, G.T.M. A Review on Zeolite Application for Aromatic Production from Non-Petroleum Carbon-Based Resources. *J. Eng. Technol. Sci.* **2023**, *55*, 131–142.
- https://doi.org/10.5614/j.eng.technol.sci.2023.55.2.3
- [16] Qazi, U.Y.; Javaid, R.; Ikhlaq, A.; Khoja, A.H.; Saleem, F. A Comprehensive Review on Zeolite Chemistry for Catalytic Conversion of Biomass/Waste into Green Fuels. *Molecules* **2022**, 27, 8578. https://doi.org/10.3390/molecules27238578
- [17] Valpotić, H.; Gračner, D.; Turk, R.; Đuričić, D.; Vince, S.; Folnožić, I.; Lojkić, M.; Žura Žaja, I.; Bedrica, L.; Maćešić, N.; *et al.* Zeolite Clinoptilolite Nanoporous Feed Additive for Animals of Veterinary Importance: Potentials and Limitations. *Periodicum Biol.* **2017**, *119*, 159–172.
- https://doi.org/10.18054/pb.v119i3.5434
- [18] Serati-Nouri, H.; Jafari, A.; Roshangar, L.; Dadashpour, M.; Pilehvar-Soltanahmadi, Y.; Zarghami, N. Biomedical Applications of Zeolite-Based Materials: A Review. *Mater. Sci. Eng. C* **2020**, *116*, 111225.
- https://doi.org/10.1016/j.msec.2020.111225
- [19] Naz, S.; Gul, A.; Zia, M.; Javed, R. Synthesis, Biomedical Applications, and Toxicity of CuO Nanoparticles. *Appl. Microbiol. Biotechnol.* **2023**, *107*, 1039–1061. https://doi.org/10.1007/s00253-023-12364-z
- [20] Yahya, N.A.A.; Samir, O.M.; Al-Ariki, S.; Ahmed, A.A.M.; Swillam, M.A. Synthesis of Novel Antibacterial Nanocomposite CuO/Ag-Modified Zeolite for Removal of MB Dye. *Sci. Rep.* **2023**, *13*, 14948. https://doi.org/10.1038/s41598-023-40790-6
- [21] Mathanmohun, M.; Sagadevan, S.; Rahman, M.Z.; Lett, J.A.; Fatimah, I.; Moharana, S.; Garg, S.; Al-Anber, M.A. Unveiling Sustainable, Greener Synthesis Strategies and Multifaceted Applications of Copper Oxide Nanoparticles. *J. Mol. Struct.* **2024**, *1305*, 137788.
- https://doi.org/10.1016/j.molstruc.2024.137788
- [22] Alswat, A.A.; Ahmad, M.B.; Hussein, M.Z.; Ibrahim, N.A.; Saleh, T.A. Copper Oxide Nanoparticles-Loaded Zeolite and its Characteristics and Antibacterial Activities. *J. Mater. Sci. Technol.* **2017**, *33*, 889–896.
- https://doi.org/10.1016/j.jmst.2017.03.015
- [23] Alangari, A.; Aboul-Soud, M.A.M.; Alqahtani, M.S.; Shahid, M.; Syed, R.; Lakshmipathy, R.; Modigunta, J.K.R.; Jaiswal, H.; Verma, M. Green Synthesis of Copper Oxide Nanoparticles Using Genus *Inula* and Evaluation of Biological Therapeutics and Environmental Applications. *Nanotechnol. Rev.* **2024**, *13*, 20240039. https://doi.org/10.1515/ntrev-2024-0039
- [24] Matei, A.; Craciun, G.; Romanitan, C.; Pachiu, C.; Tucureanu, V. Biosynthesis and Characterization of Copper Oxide Nanoparticles. *Eng. Proc.* **2023**, *37*, 54. https://doi.org/10.3390/ECP2023-14629
- [25] Alshami, H.G.A.; Al-Tamimi, W.H.; Hateet, R.R. The Antioxidant Potential of Copper Oxide Nanoparticles Synthesized from a New Bacterial Strain. *Biodiversitas* **2023**, *24*, 2666–2673. https://doi.org/10.13057/biodiv/d240519

- [26] Kamila, E.A.; Abidin, Z.; Arief, I.I.; Trivadila. Synthesis, Characterization, Antibacterial Activity, and Potential Water Filter Application of Copper Oxide/Zeolite Composite. *Makara J. Sci.* **2023**, *27*, 186–193. https://doi.org/10.7454/mss.v27i3.1555
- [27] Znak, Z.; Sukhatskiy, Y. The Brandon Method in Modelling the Cavitation Processing of Aqueous Media. *East. Eur. J. Enterp. Technol.* **2016**, *3*(8(81), 37–42. https://doi.org/10.15587/1729-4061.2016.72539
- [28] Znak, Z.O.; Sukhatskiy, Y.V.; Zin, O.I.; Khomyak, S.V.; Mnykh, R.V.; Lysenko, A.V. The Decomposition of the Benzene in Cavitation Fields. *Voprosy Khimii i Khimicheskoi Tekhnologii* **2018**, *1*, 72–77.
- [29] Znak, Z.O.; Sukhatskiy, Y.V.; Mnykh, R.V.; Tkach, Z.S. Thermochemical Analysis of Energetics in the Process of Water Sonolysis in Cavitation Fields. *Voprosy Khimii i Khimicheskoi Tekhnologii* **2018**, *3*, 64–69.
- [30] Yavorskyi, V.T.; Znak, Z.O.; Sukhatskyi, Y.V.; Mnykh, R.V. Energy Characteristics of Treatment of Corrosive Aqueous Media in Hydrodynamic Cavitators. *Mater. Sci.* **2017**, *52*, 595–600. https://doi.org/10.1007/s11003-017-9995-8
- [31] Rajamanikkam, S.C.R.R., Anbalagan, G.; Subramanian, B.; Suresh, V.; Sivaperumal, P. Green Synthesis of Copper and Copper Oxide Nanoparticles from Brown Algae *Turbinaria* Species' Aqueous Extract and its Antibacterial Properties. *Cureus* **2024**, *16*, e57366. https://doi.org/10.7759/cureus.57366
- [32] Du, B.D.; Phu, D.V.; Quoc, L.A.; Hien, N.Q. Synthesis and Investigation of Antimicrobial Activity of Cu₂O Nanoparticles/Zeolite. *J. Nanopart.* **2017**, 2017, 7056864. https://doi.org/10.1155/2017/7056864
- [33] Alswat, A.A.; Ahmad, M.B.; Saleh, T.A. Zeolite Modified with Copper Oxide and Iron Oxide for Lead and Arsenic Adsorption from Aqueous Solutions. *J. Water Supply: Res. Technol.* **2016**, *65*, 465–479.
- https://doi.org/10.2166/aqua.2016.014
- [34] Prakruthia, R.; Deepakumari, H.N. CuO Nanoparticles: Green Combustion Synthesis, Applications to Antioxidant, Photocatalytic and Sensor Studies. *RSC Adv.* **2024**, *14*, 28703. https://doi.org/10.1039/d4ra04622f
- [35] Sydorchuk, V.; Vasylechko, V.; Khyzhun, O.; Gryshchouk, G.; Khalameida, S.; Vasylechko, L. Effect of High-Energy Milling on the Structure, Some Physicochemical and Photocatalytic Properties of Clinoptilolite. *Appl. Catal. A Gen.* **2021**, *610*, 117930. https://doi.org/10.1016/j.apcata.2020.117930
- [36] Aloulou, H.; Bouhamed, H.; Ghorbel, A.; Amar, R.B.; Khemakhem, S. Elaboration and Characterization of Ceramic Microfiltration Membranes from Natural Zeolite: Application to the Treatment of Cuttlefish Effluents. *Desalin. Water Treat.* **2017**, 95, 9–17. https://doi.org/10.5004/dwt.2017.21348
- [37] Manko, N.O.; Ilkov, O.O.; Klyuchivska, O.Y.; Vasylechko, V.O.; Sydorchuk, V.V.; Kovalska, N.P.; Kostiv, O.I.; Bagday, S.R.; Zelinskiy, A.V.; Gromyko, O.M.; *et al.* Antibacterial Action of Novel Zeolite-Based Compositions Depends upon Doping with Ag⁺ and Cu²⁺ Cations. *Ukr. Biochem. J.* **2024**, *96*, 104–118, https://doi.org/10.15407/ubi96.05.104
- [38] Nikolov, A.; Dobreva, L.; Danova, S.; Miteva-Staleva, J.; Krumova, E.; Rashev, V.; Neli Vilhelmova-Ilieva, N. Natural and Modified Zeolite Clinoptilolite with Antimicrobial Properties: A Review. *Acta Microbiologica Bulgarica* **2023**, *39*, 147–161. https://doi.org/10.59393/amb23390207

- [39] Znak, Z.; Kochubei, V. Influence of Natural Clinoptilolite Modification with Ions and Zero-Valent Silver on its Sorption Capacity. *Chem. Chem. Technol.* **2023**, *17*, 646–654. https://doi.org/10.23939/chcht17.03.646
- [40] Al-Maliki, S.B.; Al-Khayat, Z.Q.; Abdulrazzak, I.A.; AlAni, A. The Effectiveness of Zeolite for the Removal of Heavy Metals from an Oil Industry Wastewater. *Chem. Chem. Technol.* **2022**, *16*, 255–258. https://doi.org/10.23939/chcht16.02.255
- [41] Kochubei, V.; Yaholnyk, S.; Bets, M.; Malovanyy, M. Use of Activated Clinoptilolite for Direct Dye-Contained Wastewater Treatment. *Chem. Chem. Technol.* **2020**, *14*, 386–393. https://doi.org/10.23939/chcht14.03.386
- [42] Konanets, R.; Stepova, K. Nonlinear Isotherm Adsorption Modelling for Copper Removal from Wastewater by Natural and Modified Clinoptilolite and Glauconite. *Chem. Technol.* **2024**, *18*, 94–102. https://doi.org/10.23939/chcht18.01.094
- [43] Milenković, J.; Hrenović, J.; Goić-Barišić, L.; Tomić, M.; Rajić, N. Antibacterial Activity of Copper-Containing Clinoptilolite/PVC Composites toward Clinical Isolate of *Acinetobacterbaumannii. J. Serb. Chem. Soc.* **2015**, *80*, 819. http://dx.doi.org/10.2298/JSC141225017M
- [44] Gebreslassie, Y.T.; Gebremeskel, F.G. Green and Cost-Effective Biofabrication of Copper Oxide Nanoparticles:

Exploring Antimicrobial and Anticancer Applications. *Biotechnol. Rep.* **2024**, *41*, e00828.

http://dx.doi.org/10.1016/j.btre.2024.e00828

Received: December 23, 2024 / Revised: April 01, 2025 / Accepted: April 17, 2025

СОНОХІМІЧНИЙ СИНТЕЗ, ХАРАКТЕРИЗАЦІЯ ТА ДОСЛІДЖЕННЯ АНТИБАКТЕРІАЛЬНОЇ АКТИВНОСТІ КОМПОЗИТУ НАНОЧАСТИНКИ ОКСИДУ МІДІ/КЛИНОПТИЛОЛІТ

Анотація. Методом сонохімічного синтезу з використанням мідного купоросу як прекурсора та натрію гідроксиду як осаджувального агента було отримано композит наночастинки СиО/клиноптилоліт. Синтезований композит було охарактеризовано техніками РД, ЕДРА, ІЧС з Фур'є-перетворенням та СЕМ. Було встановлено високу антибактеріальну активність композиту щодо грам-позитивної бактерії Staphylococcus aureus subsp. aureus ATCC 25923.

Ключові слова: сонохімічний синтез, композит наночастинки СиО/клиноптилоліт, рівняння Дебая—Шеррера, антибактеріальна активність, грам-позитивна бактерія Staphylococcus aureus.